The $\gamma^*\gamma^*$ total cross section in NLA BFKL

Dmitry Ivanov

Sobolev Institute of Mathematics, Novosibirsk

In collaboration with

Beatrice Murdaca and Alessandro Papa

Dipartimento di Fisica, Università della Calabria

Diffraction 2014, 14th September 2014

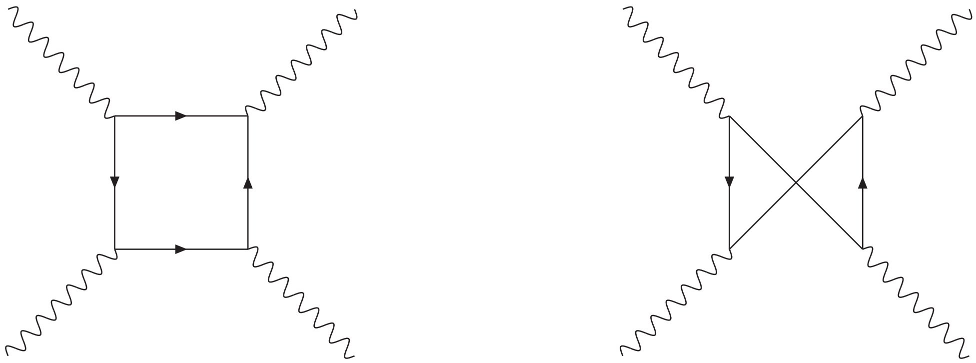

Figure 1: Quark box LO diagrams.

1 Introduction

Similarly to the e^+e^- annihilation into hadrons, the total cross section for the collision of two off-shell photons with large virtualities

$$\gamma^*(Q_1)\gamma^*(Q_2) \to X$$

is an important test ground for perturbative QCD:

- **At low energies, the dominant contribution comes from the QED quark box.**
  The resummation of double logs appearing
  in the QCD corrections – J. Bartels, M. Lublinsky [2004].
- **At higher energies, the gluon exchange in the t-channel dominates, due to the different power asymptotics for $s \to \infty$.**
  At higher orders in α_s: the terms, $\sim (\alpha_s \ln(s))^n$ (LLA), and $\sim \alpha_s(\alpha_s \ln(s))^n$ (NLA) – must be resummed.

- **LLA BFKL calculations:**
  J. Bartels, A. De Roeck, H. Lotter [1996];
  S. Brodsky, F. Hautmann, D. E. Soper [1997], ...
- **NLA BFKL with LO impact factors:**
  BLM – S.J. Brodsky, V.S. Fadin, V.T. Kim, L.N. Lipatov, G.B. Pivovarov [2002], ...
  PMS – F. Caporale, D.Yu. Ivanov, A. Papa [2008]
- **For complete NLA BFKL we need NLO impact factor!**

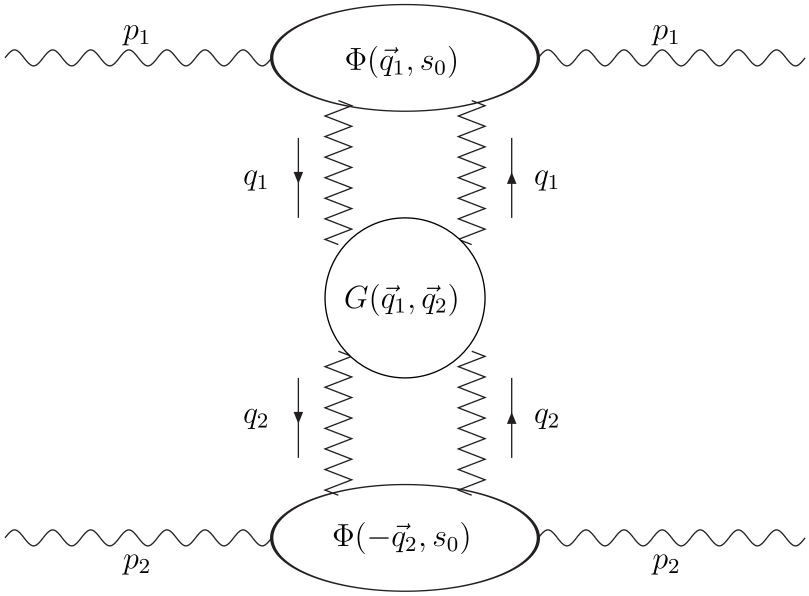

Figure 2: Schematic representation of the elastic amplitude for the $\gamma^*(p_1)\,\gamma^*(p_2)$ forward scattering.

- **in the original BFKL: works of J. Bartels and coll.**
  some final numerical results –
  J. Bartels, G. Chachamis in Proceedings of Diffraction 2006

- **in the dipole approach based on the operator expansion in Wilson lines (J. Balitsky):**
  analytic results for photon IF J. Balitsky and G. Chirilli [2013]

The $\gamma^*\gamma^*$ cross with *full* inclusion of the BFKL resummation in the NLA in dipole approach:
G. Chirilli, Yu. Kovchegov [2014].
It allows us to extract photon IF in original BFKL scheme!

What we did:

- **consider several NLA-equivalent representations of the $\gamma^*\gamma^*$ total cross section, in combination with two among the most common methods of optimization of the perturbative series, namely the principle of minimal sensitivity (PMS) and the Brodsky-Lepage-Mackenzie (BLM) method.**

- **compare our prediction with LEP2 data**

- **try to compare Bartels-Chachamis and Balitsky-Chirilli results for photon IF**

2 BFKL contribution to the $\gamma^*\gamma^*$ total cross section

LLA BFKL:

$$\sigma_{\rm tot}^{\gamma^*\gamma^*}(s,Q_1,Q_2)=\sum_{i,k=T,L}\frac{1}{(2\pi)^2Q_1Q_2}\int\limits_{-\infty}^{+\infty}d\nu\left(\frac{Q_1^2}{Q_2^2}\right)^{i\nu}F_i(\nu)F_k(-\nu)\left(\frac{s}{s_0}\right)^{\bar\alpha_s\chi(\nu)}\,,$$

where $\bar\alpha_s\equiv\alpha_s(\mu_R)N_c/\pi$, $\chi(\nu)$ is the eigenvalue of LLA BFKL equation,

$$\chi(\nu)=2\psi(1)-\psi\left(\frac{1}{2}+i\nu\right)-\psi\left(\frac{1}{2}-i\nu\right)$$

and LO photon IFs

$$F_T(\nu)=F_T(-\nu)=\alpha\,\alpha_s(\mu_R)\left(\sum_q e_q^2\right)\frac{\pi^2}{8}\frac{9+4\nu^2}{\nu\,(1+\nu^2)}\frac{\sinh(\pi\nu)}{\cosh^2(\pi\nu)}\,,$$

$$F_L(\nu)=F_L(-\nu)=\alpha\,\alpha_s(\mu_R)\left(\sum_q e_q^2\right)\frac{\pi^2}{4}\frac{1+4\nu^2}{\nu\,(1+\nu^2)}\frac{\sinh(\pi\nu)}{\cosh^2(\pi\nu)}$$

In LLA BFKL the argument of the strong and electromagnetic coupling constants, μ_R, and the value of the scale s_0 are not fixed.

NLA BFKL cross section:

similar to the NLA forward amplitude for $\gamma^*\gamma^* \to VV$: D. Ivanov, A. Papa [2006].

$$\sigma_{\rm tot}^{\gamma^*\gamma^*}(s,Q_1,Q_2,s_0,\mu_R) = \frac{1}{(2\pi)^2 Q_1 Q_2}\int\limits_{-\infty}^{+\infty} d\nu \left(\frac{Q_1^2}{Q_2^2}\right)^{i\nu}\left(\frac{s}{s_0}\right)^{\bar\alpha_s(\mu_R)\chi(\nu)}$$

$$\times \sum_{i,k=T,L} F_i(\nu)F_k(-\nu)\left\{1+\bar\alpha_s(\mu_R)\left(\frac{F_i^{(1)}(\nu,s_0,\mu_R)}{F_i(\nu)}+\frac{F_k^{(1)}(-\nu,s_0,\mu_R)}{F_k(-\nu)}\right)\right.$$
$$\left.+\bar\alpha_s^2(\mu_R)\ln\left(\frac{s}{s_0}\right)\left[\bar\chi(\nu)+\frac{\beta_0}{8N_c}\chi(\nu)\left(-\chi(\nu)+\frac{10}{3}+2\ln\frac{\mu_R^2}{Q_1Q_2}\right)\right]\right\} \,,$$

where (V. Fadin, L. Lipatov)

$$\begin{aligned}\bar\chi(\nu) &= -\frac{1}{4}\left[\frac{\pi^2-4}{3}\chi(\nu)-6\zeta(3)-\chi''(\nu)-\frac{\pi^3}{\cosh(\pi\nu)}\right.\\ &+ \left.\frac{\pi^2\sinh(\pi\nu)}{2\,\nu\,\cosh^2(\pi\nu)}\left(3+\left(1+\frac{n_f}{N_c^3}\right)\frac{11+12\nu^2}{16(1+\nu^2)}\right)+4\,\phi(\nu)\right]\,,\end{aligned}$$

$$\phi(\nu) = 2\int\limits_0^1 dx\,\frac{\cos(\nu\ln(x))}{(1+x)\sqrt{x}}\left[\frac{\pi^2}{6}-\mathbf{Li}_2(x)\right]\,,\qquad \mathbf{Li}_2(x) = -\int\limits_0^x dt\,\frac{\ln(1-t)}{t}\,,$$

n_f is the number of active quarks, $F_{L,T}^{(1)}(\nu,s_0,\mu_R)$ are the NLO corrections to the longitudinal/transverse photon impact factor in the ν-representation and

$$\beta_0 = \frac{11}{3}N_c - \frac{2}{3}n_f\,.$$

Comparison with Chirilli-Kovchegov result:

$$
\begin{aligned}
\sigma_{TT}^{(\mathrm{CK})} &= \left(\sum_q e_q^2\right)^2 \frac{\alpha^2\alpha_s^2}{Q_1 Q_2}\frac{\pi^2}{2^8}\int_{-\infty}^{+\infty} d\nu \left(\frac{Q_1^2}{Q_2^2}\right)^{i\nu}\left(\frac{s}{Q_1 Q_2}\right)^{\bar{\alpha}_s\chi(\nu)+\bar{\alpha}_s^2\chi^{(1)}(\nu)} \\
&\times \left[\frac{(9+4\nu^2)}{\nu\,(1+\nu^2)}\frac{\sinh(\pi\nu)}{\cosh^2(\pi\nu)}\right]^2 \left[1+\frac{\alpha_s}{\pi}+\frac{\bar{\alpha}_s}{2}\mathcal{F}_1(\nu)\right]\left[1+\frac{\alpha_s}{\pi}+\frac{\bar{\alpha}_s}{2}\mathcal{F}_1(-\nu)\right] \\
&\times \left\{1+\bar{\alpha}_s\Re\left[F(\nu)\right]\right\} ,
\end{aligned}
$$

with

$$
\chi^{(1)}(\nu) = \bar{\chi}(\nu) + \frac{\beta_0}{8N_c}\chi(\nu)\left(-\chi(\nu)+\frac{10}{3}\right) .
$$

and additional factor :

$$
\left\{1+\bar{\alpha}_s\Re\left[F(\nu)\right]\right\}
$$

originates from QCD correction to elementary dipole-dipole scattering in Balitsky approach.

Extracted photon IFs:

$$
\begin{aligned}
\frac{F_T^{(1)}(\nu, s_0, \mu_R)}{F_T(\nu)} &= \frac{\chi(\nu)}{2}\ln\frac{s_0}{Q^2} + \frac{\beta_0}{4N_c}\ln\frac{\mu_R^2}{Q^2} \\
&+ \frac{3C_F}{4N_c} - \frac{5}{18}\frac{n_f}{N_c} + \frac{\pi^2}{4} + \frac{85}{36} - \frac{\pi^2}{\cosh^2(\pi\nu)} - \frac{4}{1+4\nu^2} + \frac{6\chi(\nu)}{9+4\nu^2} \\
&+ \frac{1}{2(1-2i\nu)} - \frac{1}{2(1+2i\nu)} - \frac{7}{18(3+2i\nu)} + \frac{20}{3(3+2i\nu)^2} - \frac{25}{18(3-2i\nu)} \\
&+ \frac{1}{2}\chi(\nu)\left[\psi\left(\frac{1}{2}-i\nu\right) + 2\psi\left(\frac{3}{2}-i\nu\right) - 2\psi(3-2i\nu) - \psi\left(\frac{5}{2}+i\nu\right)\right]
\end{aligned}
$$

and

$$
\begin{aligned}
\frac{F_L^{(1)}(\nu, s_0, \mu_R)}{F_L(\nu)} &= \frac{\chi(\nu)}{2}\ln\frac{s_0}{Q^2} + \frac{\beta_0}{4N_c}\ln\frac{\mu_R^2}{Q^2} \\
&+ \frac{3C_F}{4N_c} - \frac{5}{18}\frac{n_f}{N_c} + \frac{\pi^2}{4} + \frac{85}{36} - \frac{\pi^2}{\cosh^2(\pi\nu)} - \frac{8(1+4i\nu)}{(1+2i\nu)^2(1-2i\nu)(3+2i\nu)} \\
&+ \frac{4}{3-4i\nu+4\nu^2}\chi(\nu) \\
&+ \frac{1}{2}\chi(\nu)\left[\psi\left(\frac{1}{2}-i\nu\right) + 2\psi\left(\frac{3}{2}-i\nu\right) - 2\psi(3-2i\nu) - \psi\left(\frac{5}{2}+i\nu\right)\right] .
\end{aligned}
$$

the dependencies on the renormalization and energy scales, are restored by the requirement that the BFKL cross section does not depend on s_0 and μ_R with NLA accuracy.

3 Numerical analysis

The kinematic range relevant for the OPAL and L3 experiments at LEP2:

- $Q_1 = Q_2 \equiv Q$, with Q^2=17 GeV^2
- the energy range $Y = 2 \div 6$, where $Y \equiv \ln(s/Q^2)$.

Strategy:

- to consider several representations of the NLA $\gamma^*\gamma^*$ total cross section, which differ one from the other only by terms beyond the NLA.
- to consider two different methods of optimization of perturbative series

We will consider two alternative procedures to fix the energy scales:

- inspired by the PMS optimization method (Stevenson):
  for each value of the center-of-mass energy s and of the virtualities of the colliding photons, we choose as optimal scales s_0 and μ_R those for which the given representation of the NLA cross section exhibits the minimum sensitivity under variation of these scales.
- inspired by the BLM method:
  again, for fixed s and photon virtualities, we perform a finite renormalization to a momentum (MOM) scheme and then choose the renormalization scale μ_R in order to remove the β_0-dependent part in the given representation of the NLA cross section, while keeping the scale s_0 fixed at the natural value Q_1Q_2. In fact, there is some freedom in implementing the BLM optimization in this context and in the following we consider two different variants, dubbed (a) and (b).

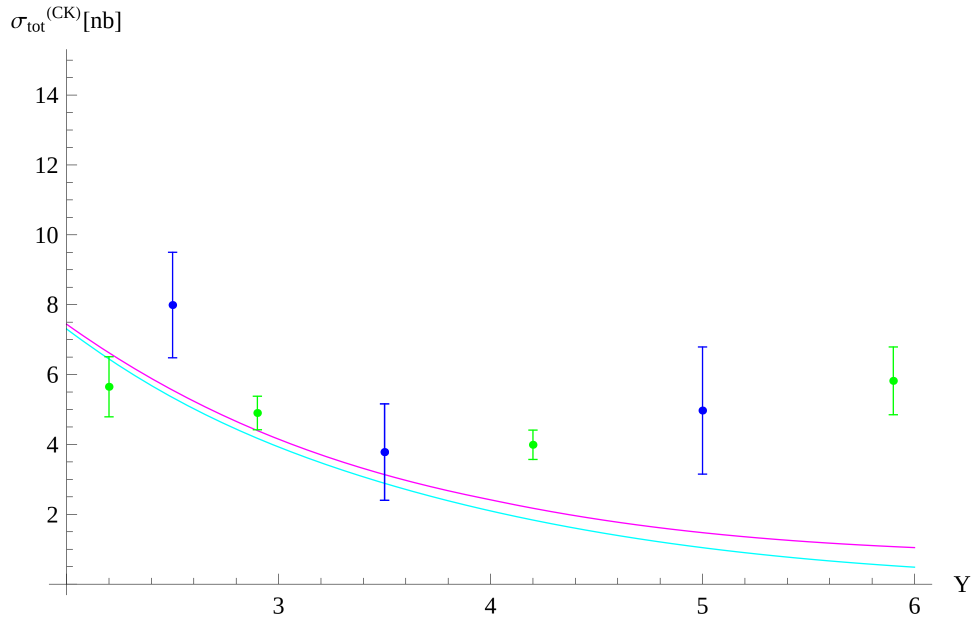

Figure 3: $\sigma_{\rm tot}^{\rm (CK)}$ *versus* Y at $Q^2 = 17$ GeV^2 ($n_f = 4$) (magenta line), together with the experimental data from OPAL (blue points, $Q^2 = 18$ GeV^2) and L3 (green points, $Q^2 = 16$ GeV^2); the cyan line represents the LO quark box contribution only.

3.1 Chirilli-Kovchegov representation

$$\sigma_{\rm tot}^{\rm (CK)}(s,Q) = \sigma_{TT}^{\rm (CK)} + \sigma_{LL}^{\rm (CK)} + \sigma_{TL}^{\rm (CK)} + \sigma_{LT}^{\rm (CK)} + \sigma_{\rm LO\ \ box}\ ,$$

where we have included the LO contribution from the quark box and contributions of different polarization states of virtual photons.

We see that the original Chirilli-Kovchegov representation for the cross section (at natural values of the scales, $s_0 = \mu_R^2 = Q^2$) gives a very small BFKL contribution and does not agree well with data above $Y = 4$.

Table 1: Values of $\sigma_{\rm tot}^{\rm (series)}$ for several values of Y at $Q^2 = 17$ GeV^2; the last two columns give the optimal values of the renormalization and energy scales.

Y	$\sigma_{\rm tot}^{\rm (series)}$[nb]	μ_R/Q	Y_0
2	7.3141	18	1
3.5	3.1095	10	3
4.5	1.9187	10	4
6	1.1909	16	5

3.2 Series representation with PMS optimization

has the advantage of making manifest the BFKL resummation of leading and subleading energy logarithms and is very practical in numerical computations.

$$\sigma_{\rm tot}^{\rm (series)}(s,Q) = \sigma_{TT}^{\rm (series)} + \sigma_{LL}^{\rm (series)} + \sigma_{TL}^{\rm (series)} + \sigma_{LT}^{\rm (series)} + \sigma_{\rm LO\ box}\ ,$$

where for $i,k = L,T$

$$Q^2\sigma_{ik}^{\rm (series)} = \frac{1}{(2\pi)^2}\left\{b_0^{ik} + \sum_{n=1}^{\infty}\bar\alpha_s\left(\mu_R\right)^n b_n^{ik}\left[\left(Y-Y_0\right)^n + d_n^{ik}\left(s_0,\mu_R\right)\left(Y-Y_0\right)^{n-1}\right]\right\}\ ,$$

with $Y_0 \equiv \ln(s_0/Q^2)$ **and**

$$b_n^{ik} = \int_{-\infty}^{+\infty} d\nu F_i\left(\nu\right)F_k\left(-\nu\right)\frac{\chi^n\left(\nu\right)}{n!}\ ,$$

$$\begin{aligned} d_n^{ik} &= n\ln\frac{s_0}{Q^2} + \frac{\beta_0}{4N_c}\left[\frac{b_{n-1}^{ik}}{b_n^{ik}}\left((n+1)\ln\frac{\mu_R^2}{Q^2} + \frac{5}{3}\left(n-1\right)\right) - \frac{n\left(n-1\right)}{2}\right] \\ &+ \frac{1}{b_n^{ik}}\int_{-\infty}^{+\infty} d\nu\, F_i\left(\nu\right)F_k\left(-\nu\right)\left[\frac{\chi^{n-1}\left(\nu\right)}{(n-1)!}\left(\frac{\bar F_i^{(1)}(\nu)}{F_i(\nu)} + \frac{\bar F_k^{(1)}(-\nu)}{F_k(-\nu)}\right) + \frac{\chi^{n-2}\left(\nu\right)}{(n-2)!}\bar\chi\left(\nu\right)\right]\ , \end{aligned}$$

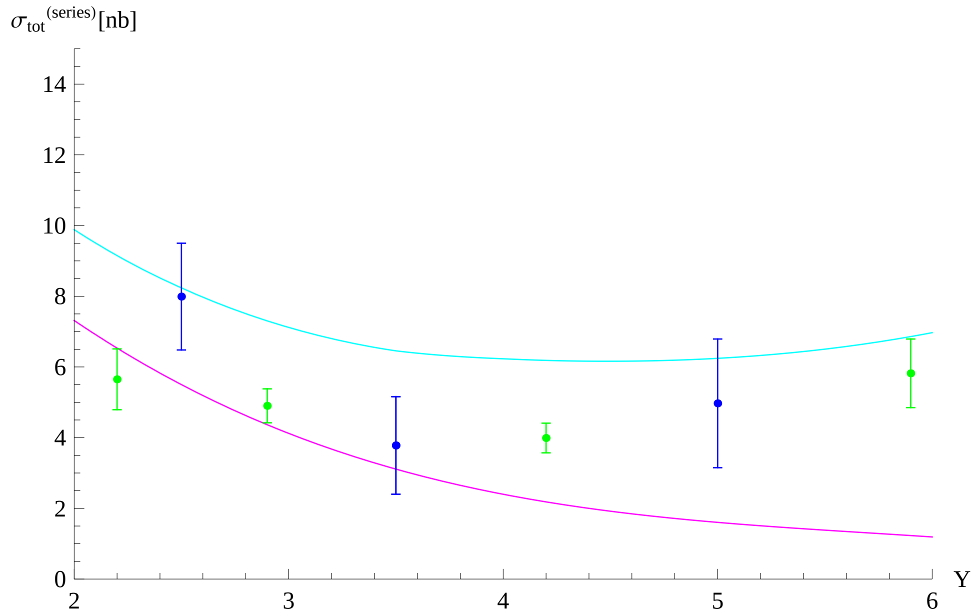

Figure 4: $\sigma_{\rm tot}^{\rm (series)}$ *versus* Y at $Q^2 = 17$ GeV^2 ($n_f = 4$) (magenta line), together with the experimental data from OPAL (blue points, $Q^2 = 18$ GeV^2) and L3 (green points, $Q^2 = 16$ GeV^2); the cyan line represents the result of Caporale, Ivanov, Papa [2008].

Table 2: Values of $\sigma_{\rm tot}^{\rm (exp,\ 1,2)}$ for several values of Y at $Q^2 = 17$ GeV^2; the columns 3-4 and 6-7 give the optimal values of the renormalization and energy scales.

Y	$\sigma_{\rm tot}^{\rm (exp,\ 1)}$[nb]	μ_R/Q	Y_0	$\sigma_{\rm tot}^{\rm (exp,\ 2)}$[nb]	μ_R/Q	Y_0
2	7.36281	18	1	7.57706	8	1
3.5	3.23512	18	3	3.25243	8	1
4.5	1.98923	18	4	1.9419	8	1
6	1.20222	18	5	1.09588	8	1

3.3 Exponential representation with PMS optimization

where the NLO corrections to the kernel are exponentiated,
in two options,
which differ by a subleading term given by the product of the two NLO corrections of the photon impact factors:

$$\sigma_{\rm tot}^{\rm (exp,\ 1)}(s,Q) = \sigma_{TT}^{\rm (exp,\ 1)} + \sigma_{LL}^{\rm (exp,\ 1)} + \sigma_{TL}^{\rm (exp,\ 1)} + \sigma_{LT}^{\rm (exp,\ 1)} + \sigma_{\rm LO\ \ box}\ ,$$

and

$$\sigma_{\rm tot}^{\rm (exp,\ 2)}(s,Q) = \sigma_{TT}^{\rm (exp,\ 2)} + \sigma_{LL}^{\rm (exp,\ 2)} + \sigma_{TL}^{\rm (exp,\ 2)} + \sigma_{LT}^{\rm (exp,\ 2)} + \sigma_{\rm LO\ \ box}\ ,$$

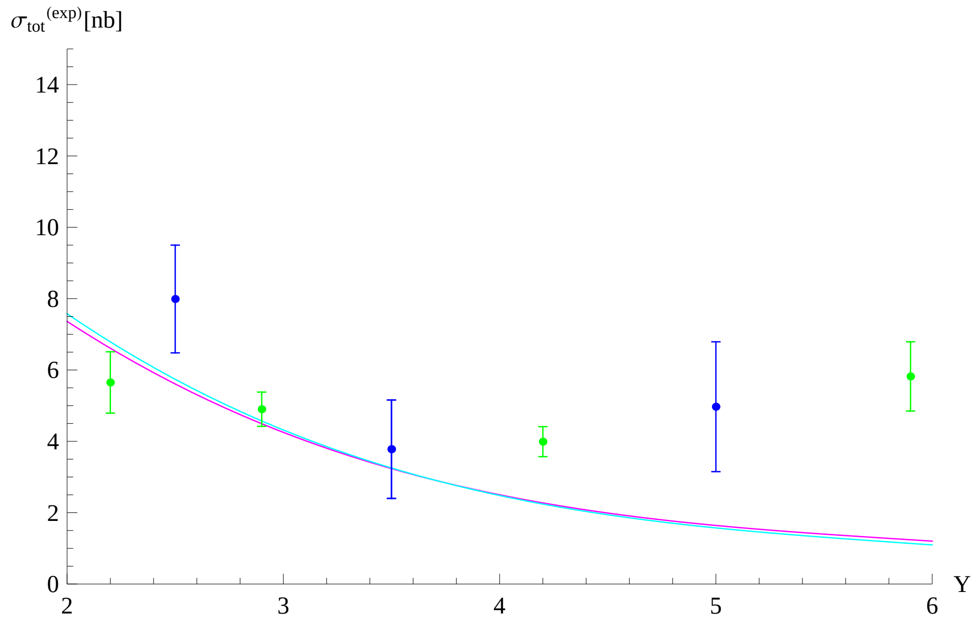

Figure 5: $\sigma_{\rm tot}^{(\rm exp,\ 1)}$ (magenta line) and $\sigma_{\rm tot}^{(\rm exp,\ 2)}$ (cyan line) *versus* Y at $Q^2 = 17$ GeV^2 ($n_f = 4$), together with the experimental data from OPAL (blue points, $Q^2 = 18$ GeV^2) and L3 (green points, $Q^2 = 16$ GeV^2).

with

$$\begin{aligned}
\sigma_{ik}^{(\rm exp,1)} &= \frac{1}{(2\pi)^2 Q^2} \int_{-\infty}^{+\infty} e^{(Y-Y_0)\left[\bar{\alpha}_s(\mu_R)\left(1+\frac{\bar{\alpha}_s(\mu_R)\beta_0}{4N_c}\ln\frac{\mu_R^2}{Q^2}\right)\chi(\nu)+\bar{\alpha}_s^2(\mu_R)\chi^{(1)}(\nu)\right]} \\
&\times \; F_i(\nu)F_k(-\nu)\left[1+\bar{\alpha}_s\left(\mu_R\right)\left(\frac{F_i^{(1)}(\nu)}{F_i(\nu)}+\frac{F_k^{(1)}(-\nu)}{F_k(-\nu)}\right)\right]
\end{aligned}$$

and

$$\begin{aligned}
\sigma_{ik}^{(\rm exp,2)} &= \frac{1}{(2\pi)^2 Q^2} \int_{-\infty}^{+\infty} e^{(Y-Y_0)\left[\bar{\alpha}_s(\mu_R)\left(1+\frac{\bar{\alpha}_s(\mu_R)\beta_0}{4N_c}\ln\frac{\mu_R^2}{Q^2}\right)\chi(\nu)+\bar{\alpha}_s^2(\mu_R)\chi^{(1)}(\nu)\right]} \\
&\times \; F_i(\nu)F_k(-\nu)\left[1+\bar{\alpha}_s\left(\mu_R\right)\left(\frac{F_i^{(1)}(\nu)}{F_i(\nu)}+\frac{F_k^{(1)}(-\nu)}{F_k(-\nu)}\right)\right. \\
&+ \; \left.\bar{\alpha}_s^2\left(\mu_R\right)\left(\frac{F_i^{(1)}(\nu)}{F_i(\nu)}\frac{F_k^{(1)}(-\nu)}{F_k(-\nu)}\right)\right] .
\end{aligned}$$

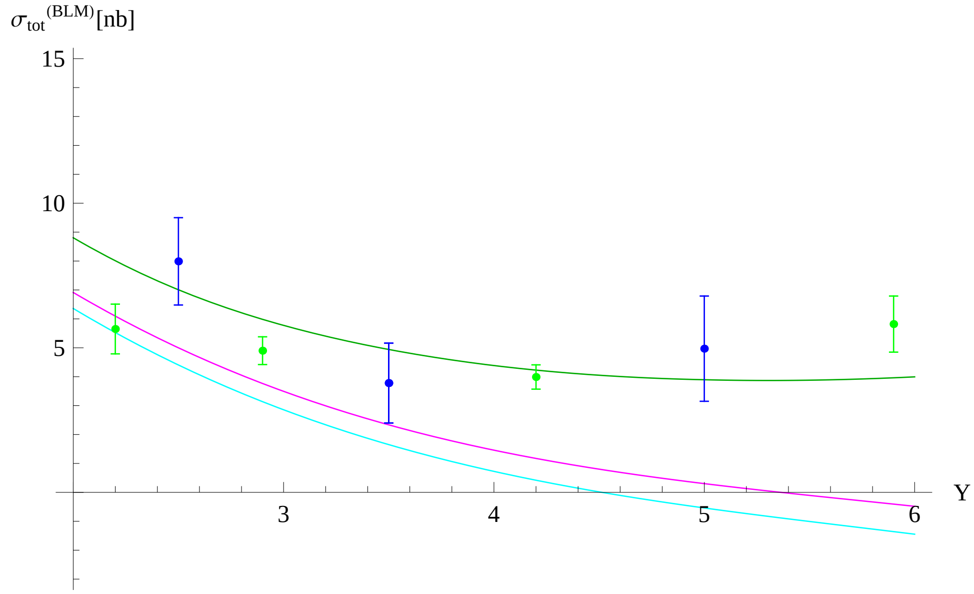

Figure 6: $\sigma_{\rm tot}^{\rm (BLM,\ a)}$ (cyan line) and $\sigma_{\rm tot}^{\rm (BLM,\ b)}$ (magenta line) *versus* Y at $Q^2 = 17$ GeV^2 ($n_f = 4$), together with the experimental data from OPAL (blue points, $Q^2 = 18$ GeV^2) and L3 (green points, $Q^2 = 16$ GeV^2); the green line represents the result of Caporale, Ivanov, Papa [2008].

3.4 Exponential representation with BLM optimization

To options for BLM scale setting (for details see Beatrice M. talk):

$$\left(\mu_{R,a}^{\rm BLM}\right)^2 = Q^2 \;\exp\left[2\left(1+\frac{2}{3}I\right)-\frac{5}{3}\right] \;,$$

and

$$\left(\mu_{R,b}^{\rm BLM}\right)^2 = Q^2 \;\exp\left[2\left(1+\frac{2}{3}I\right)-\frac{5}{3}+\frac{1}{2}\chi\left(\nu\right)\right] \;.$$

4 Discussion

We found:

- the account of the Balitsky and Chirilli expression for NLO photon impact factor reduces the BFKL contribution to the cross section to very small values.
- it makes impossible to describe LEP2 data as a sum of BFKL and LO QED quark box contributions!!!

What does it mean?

- Perhaps, even at such high energies the BFKL contribution could be still not the dominant one in comparison with terms which are suppressed by powers of the energy $\sim 1/s$
- the LO QED quark box:
  itself receives, at higher QCD orders, large corrections enhanced by double logs. Their resummation is important (Bartels-Lublinsky) and leads to a considerable enhancement of the quark box contribution. But still, these effects are not large enough for a good description of LEP2 data at $Y = 3.5 \div 6$ without a sizable BFKL contribution.
- Other, not taken into account subleading terms:
  In particular, terms, subleading in energy, coming from diagrams with gluon exchange in the t-channel can be important.

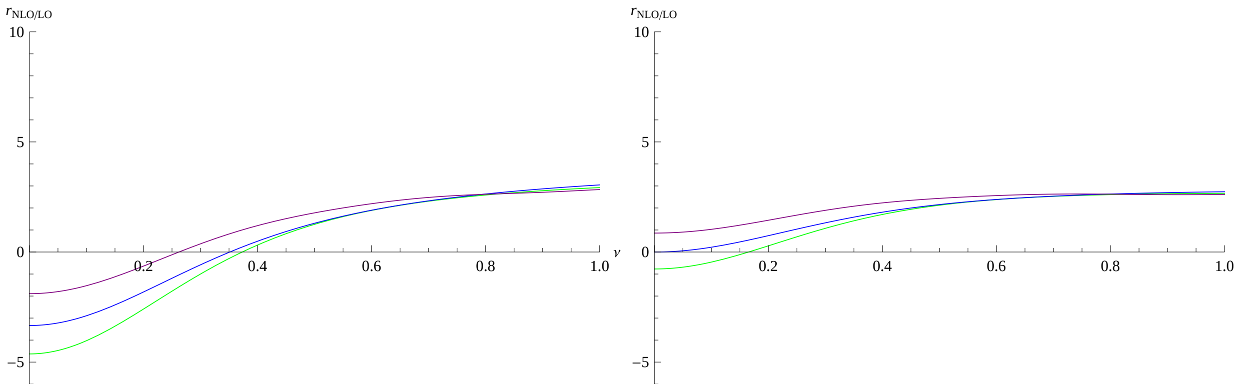

Figure 7: Behavior of $r^T_{\rm NLO/LO}(\nu, s_0, \mu_R)$ (green), $r^L_{\rm NLO/LO}(\nu, s_0, \mu_R)$ (blue) and $r^{\rm (mesons)}_{\rm NLO/LO}(\nu, s_0, \mu_R)$ (violet) for the following cases: $Q^2 = \mu_R^2 = 17$ GeV^2, $Y_0 = 0$ on the left and $Q^2 = 17$ GeV^2, $\mu_R^2 = (10Q)^2$, $Y_0 = 2.2$ on the right.

Several comments related to IFs:

- **the NLO corrections to IF are very large indeed:**

$$r^{(T,L)}_{\rm NLO/LO}(\nu, s_0, \mu_R) \equiv 1 + \bar{\alpha}_s(\mu_R)\left(\frac{F^{(1)}_{T,L}(\nu, s_0, \mu_R)}{F_{T,L}(\nu)} + \frac{F^{(1)}_{T,L}(-\nu, s_0, \mu_R)}{F_{T,L}(-\nu)}\right) .$$

For comparison, we consider also the similar quantity $r^{\rm (mesons)}_{\rm NLO/LO}$ for IF $\gamma^* \to V$ which appeared in the description of $\gamma^*\gamma^* \to VV$ to two light vector mesons (D. Ivanov, M. Kotsky, A. Papa)

$$r^{\rm (mesons)}_{\rm NLO/LO}(\nu, s_0, \mu_R) \equiv 1 + \bar{\alpha}_s(\mu_R)\left(\frac{c_1^{(1)}(\nu, s_0, \mu_R)}{c_1(\nu)} + \frac{c_2^{(1)}(-\nu, s_0, \mu_R)}{c_2(-\nu)}\right) .$$

- **Color structure of IF:**

$$IF_{NLA} = N_c A + \frac{1}{N_c} B + n_f C$$

Contrary to other cases ($\gamma^* \to V$, Mueller-Navelet jet vertex, ...) Balitsky-Chirilly IF has very simple subleading $\sim 1/N_c$ contributions (QCD correction to γ^* vertex).
Does it means that Balitsky-Chirilly results actually derived in large N_c limit?

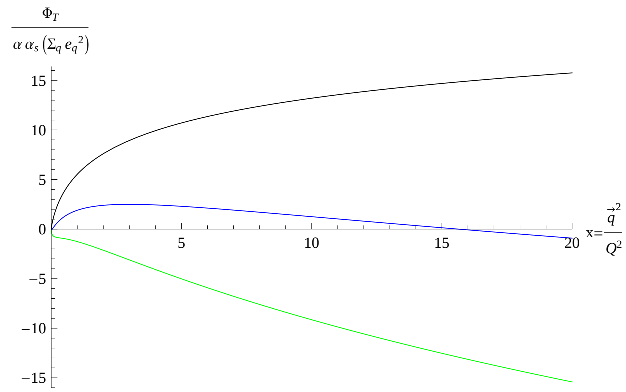

Figure 8: Behavior of the photon impact factor (the transverse polarization) with the Reggeon transverse momentum $\vec{q}$, through the variable $x \equiv \vec{q}^2/Q^2$. The black curve represents the LO impact factor, the green curve the sum of LO and NLO parts and the blue curve the same as the green curve, but with the NLO part reduced by the factor 1.87.

Balitsky-Chirilli vs Bartels-Chachamis results:

we need to transfer the photon impact factor from the ν- to the transverse momentum representation:

$$\Phi_T(x, s_0, \mu_R) = \int_{-\infty}^{\infty} d\nu \frac{(x)^{-i\nu+\frac{1}{2}}}{\pi\sqrt{2}} \left[F_T(\nu) + \bar{\alpha}_s(\mu_R) F_T^{(1)}(\nu, s_0, \mu_R)\right] ,$$

where $x \equiv \vec{q}^2/Q^2$.

**We present results for $\Phi_T(x, s_0, \mu_R)/(\alpha\,\alpha_s \left(\sum_q e_q^2\right))$,
where we used: $s_0 = 10$ GeV^2 , $Q^2 = \mu_R^2 = 15$ GeV^2; moreover, we take $n_f = 1$ and $\alpha_s = 0.177206$. [thanks to Grigorios Chachamis for this information about n_f and α_s]**

- **Comparing the shape of the x-dependence with the NLO curves in of Bartels-Chachamis, we should conclude that the results of Balitsky-Chirilli are not in agreement with those one of Bartels-Chachamis.**
- **Interestingly, a qualitative agreement between Balitsky-Chirilli and Bartels-Chachamis resuls for the x-shape of $\Phi(x, s_0, \mu_R)$ could be obtained only if the NLO part of Balitsky-Chirilli IF is reduced by the factor ~ 1.87.**